

Measuring size dependent electrical properties from nanoneedle structures: Pt/ZnO Schottky diodes

Shimin Mao, Tao Shang, Byoungnam Park, Daniel D. Anderson, and Shen J. Dillon

Citation: [Appl. Phys. Lett. **104**, 153105 \(2014\)](#);

View online: <https://doi.org/10.1063/1.4871509>

View Table of Contents: <http://aip.scitation.org/toc/apl/104/15>

Published by the [American Institute of Physics](#)

Articles you may be interested in

[Pt / ZnO nanowire Schottky diodes](#)

Applied Physics Letters **85**, 3107 (2004); 10.1063/1.1802372

[Extraction of Schottky diode parameters from forward current-voltage characteristics](#)

Applied Physics Letters **49**, 85 (1998); 10.1063/1.97359

[Effects of substrate and anode metal annealing on InGaZnO Schottky diodes](#)

Applied Physics Letters **110**, 011602 (2017); 10.1063/1.4973693

[ZnO Schottky barriers and Ohmic contacts](#)

Journal of Applied Physics **109**, 121301 (2011); 10.1063/1.3581173

[Direct measurement of defect and dopant abruptness at high electron mobility ZnO homojunctions](#)

Applied Physics Letters **109**, 143506 (2016); 10.1063/1.4963888

[A modified forward I-V plot for Schottky diodes with high series resistance](#)

Journal of Applied Physics **50**, 5052 (2008); 10.1063/1.325607



Measuring size dependent electrical properties from nanoneedle structures: Pt/ZnO Schottky diodes

Shimin Mao,^{1,a)} Tao Shang,^{2,a)} Byoungnam Park,^{1,3} Daniel D. Anderson,¹ and Shen J. Dillon^{1,2,b)}

¹*Department of Materials Science and Engineering, University of Illinois at Urbana-Champaign, Urbana, Illinois 61801, USA*

²*Frederick Seitz Materials Research Laboratory, University of Illinois at Urbana-Champaign, Urbana, Illinois 61801, USA*

³*Department of Materials Science and Engineering, Hongik University, 72-1 Sangsu-dong, Mapo-gu, Seoul 121-791, Korea*

(Received 4 March 2014; accepted 4 April 2014; published online 15 April 2014)

This work reports the fabrication and testing of nanoneedle devices with well-defined interfaces that are amenable to a variety of structural and electrical characterization, including transmission electron microscopy. Single Pt/ZnO nanoneedle Schottky diodes were fabricated by a top down method using a combination of electro-polishing, sputtering, and focused ion beam milling. The resulting structures contained nanoscale planar heterojunctions with low ideality factors, the dimensions of which were tuned to study size-dependent electrical properties. The diameter dependence of the Pt/ZnO diode barrier height is explained by a joule heating effect and/or electronic inhomogeneity in the Pt/ZnO contact area. © 2014 AIP Publishing LLC. [<http://dx.doi.org/10.1063/1.4871509>]

Nanostructured ZnO has been of interest for potential applications as UV light-emitters, gas sensors, surface acoustic wave devices, and transparent thin-film transistors.^{1–9} In recent years, the electrical properties of 1D ZnO nanostructures have attracted interest for a number of applications such as diodes,^{10–12} photovoltaics,^{13–15} and sensors,^{16,17} due to their low cost, unique properties, and compatibility with Si-based materials. Particularly, the electrical and structural properties of the heterogeneous interface between ZnO and various inorganic materials have been extensively researched.^{18–20} To probe the effects of embedded interfaces in ZnO, 1D devices have been fabricated by a number of methods including e-beam lithography and solvent-based processing.^{21,22} Few techniques produce well-defined planar heterojunction interfaces between the pristine ZnO and various inorganic counterparts. Additionally, the arrangements of many 1D test structures are not amenable to perform electrical and structural (e.g., Scanning Electron Microscopy (SEM), Transmission Electron Microscopy (TEM), optical, spectroscopy, etc.) characterization on isolated individual nanowires.

Here, a clearly defined ZnO/Pt planar-junction was fabricated and demonstrated as an electrical probe for studying charge injection and transport in a diode structure that can simultaneously be characterized via TEM. Furthermore, we demonstrate the use of the nanoneedle structure for measuring size-dependent electrical properties ranging between the nano- and micro-scale.

A Pt/ZnO nanoneedle diode was fabricated on a bulk Mo wire (diameter 100 μm, Goodfellow Inc., 99.95%), as shown in Figure 1(a). The wire was initially electro-polished in NaOH solution (5 wt. %) for 25 s under 5 V applied bias. The wire was mounted in a Cu tube to support it during

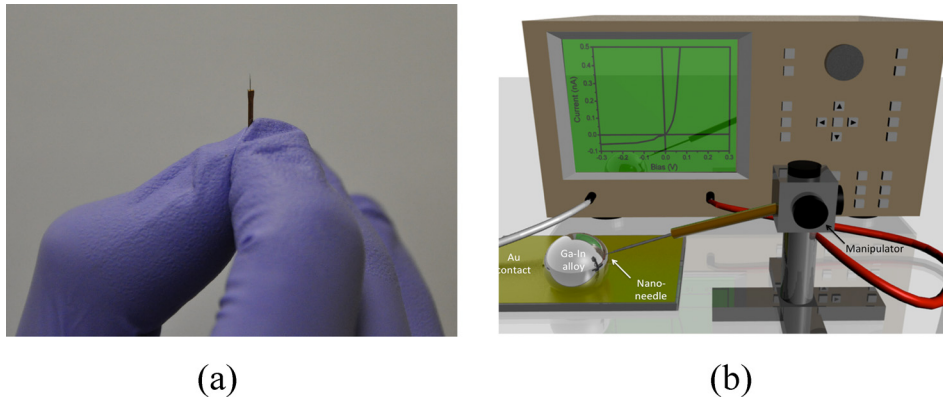
subsequent manipulation. A focused ion beam (FIB, FEI DB 235) milled the top surface in order to produce a flat region approximately 10 μm in diameter. A 100 nm Pt thin film was deposited onto this surface by magnetron sputtering (AJA international, ATC 1300) with a base pressure of 10^{–7} Torr at room temperature. An 800 nm thick ZnO film was grown on the Pt thin film via pulsed-laser deposition (PLD) using a KrF excimer laser (Coherent, LPX 205) at room temperature with an oxygen pressure of 20 mTorr, laser fluence of 0.14 J/cm², and frequency of 3 Hz. ZnO is an n-type semiconductor due to the intrinsic oxygen defects evolved during PLD growth.²³ A thick film of Al (1.2 μm) was sputtered on top to serve as the Ohmic contact.^{24,25} The 1D nanoneedle was then prepared by a multi-step annular FIB milling procedure.

The Pt/ZnO nanoneedle was tested in the configuration depicted in Figure 1(b). All *I*-*V* measurements were performed using an RF-1 Probe Station (Cascade Microtech, Inc) and a 4155c Semiconductor Parameter Analyzer (Agilent Technologies, Inc.). A Ga-In alloy (Ga: 25 wt. %, In: 75 wt. %) droplet was placed on a Au electrode that was maintained at 40 °C. The macroscopically supported nanoneedle was attached to a micromanipulator and contacted to the Ga-In droplet under an optical microscope. The high surface tension of the Ga-In droplet prevented its wetting of the nanoneedle, which would short the circuit.

The structure of the nanoneedle devices can be directly imaged in the TEM. Figure 2 depicts a Z-contrast scanning transmission electron microscopy (STEM) image of the Pt/ZnO interface. It shows a 200 nm diameter Pt/ZnO heterojunction interface with a well-defined planar interface. The diameter of the nanoneedle was measured directly, and a tilt series was utilized to ensure that the cross-section is approximately circular. Selected area electron diffraction indicates that the ZnO is single crystalline and grows along the (0001) orientation. No Ga peak was observed in energy dispersive

^{a)}S. Mao and T. Shang contributed equally to this work.

^{b)}Electronic mail: sdillon@illinois.edu



X-ray spectroscopy (EDS), suggesting that any existing Ga contamination from the ion beam milling is below the detectable limit ($\sim 1\%$).

To examine charge injection and transport phenomena at the Pt/ZnO interface in the diode structure, electrical tests were performed in the manner described above. From the I - V curve in Figure 3(a), it is shown that the nanoneedle diode exhibits rectifying behavior, which is consistent with published findings of Pt/ZnO diodes.¹¹ The turn-on voltage was approximately 0.35 V with a reverse-bias breakdown at -2 V, as seen in the inset of Figure 3(a). The total current consists of thermionic emission and tunneling currents. However, due to the reasonably high mobility and shallow impurity energy level of the ZnO produced through pulsed laser deposition,²⁶ the tunneling current can be ignored.²⁷ Therefore, the I - V curves are dominated by thermionic-field emission in the forward bias regime as shown in Figure 3(b). Here, assuming that thermionic emission is the predominant mechanism, the junction current for a Schottky barrier is described by

$$I = I_0 \left[\exp \left(\frac{q(V - IR_s)}{nkT} \right) - 1 \right],$$

where the saturation current I_0 is described by

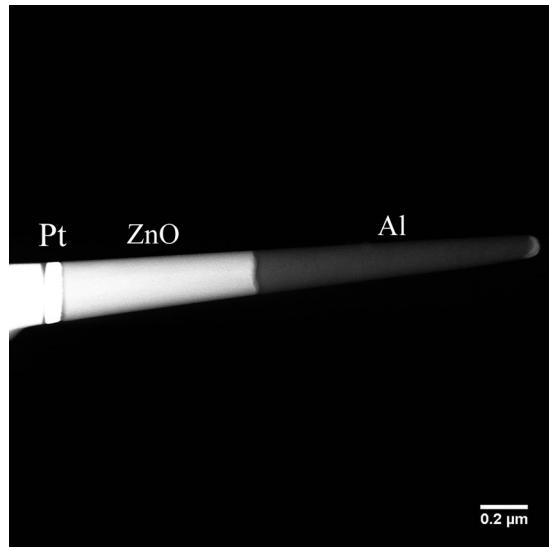


FIG. 2. Z-contrast STEM image of a Pt/ZnO nanoneedle Schottky diode.

FIG. 1. (a) Image of a Pt/ZnO nanoneedle structure and (b) schematic diagram of the test set-up.

$$I_0 = A^* AT^2 \exp \left(- \frac{q\Phi_b}{kT} \right),$$

where A^* is the Richardson constant for ZnO, A is the area of the diode, Φ_b is the barrier height, and R_s is the series resistance. The Richardson constant of ZnO was chosen to be its theoretical value, which is $32 \text{ A cm}^{-2} \text{ K}^{-2}$.²⁷ The diode area, A , can be measured precisely using the electron microscopy images (see Figure 2). T is chosen to be the ambient temperature during testing, 313 K , which may not necessarily be the actual temperature if Joule heating is significant. A general fitting method from Cheung²⁸ was applied, the calculated barrier height Φ_b and ideality factor n for the 200 nm nanoneedle, were 0.47 eV and 1.11 , respectively. This small ideality factor suggests a low density of bulk and interface traps at the Pt/ZnO interface.

The barrier height of the 200 nm diameter diode is rather small in comparison with the theoretical bulk value.²⁹ Interestingly, the low barrier height of our nanoneedle diode is consistent with previous studies for nanowire ZnO-Pt Schottky diode¹⁰ and other micro-scale diodes.^{27,30} To probe the size effect systematically, 500 nm and $3 \mu\text{m}$ Pt/ZnO diodes were also fabricated using the same method. The inset of Figure 4(a) shows the SEM images of Pt/ZnO Schottky diodes of different sizes. The I - V curves for diodes with three different diameters, under forward bias, are plotted on a logarithmic scale as shown in Figure 4(a). As the size increases, the current density decreases, which indicates that the barrier height increases with the increasing size. The calculated barrier height for 200 nm , 500 nm , and $3 \mu\text{m}$ diodes are 0.470 , 0.504 , and 0.548 eV , respectively. In order to test reproducibility of the experiment, several $3 \mu\text{m}$ samples were identically fabricated. The calculated barrier heights were $0.553 \pm 0.012 \text{ eV}$, which demonstrate the reproducibility of the approach.

The barrier heights from our experiments are compared with published data in Figure 4(b). It shows that the barrier height consistently increases with the size of the diode. The origins of this behavior can be attributed to two main factors: Barrier inhomogeneity and the Joule heating effect. Electronic inhomogeneity over the Pt/ZnO contact area can decrease the barrier height. The real barrier height can be expressed by $\Phi_R = \Phi_{bo} - \frac{q\sigma_0^2}{2kT}$, where σ_0 is the barrier homogeneity ($\sigma_0 = 0$ when the barrier height is completely homogeneous). As σ_0 decreases, the real barrier height increases. In other words, the barrier homogeneity is more predominant in diodes with large cross-sectional area than small ones, leading

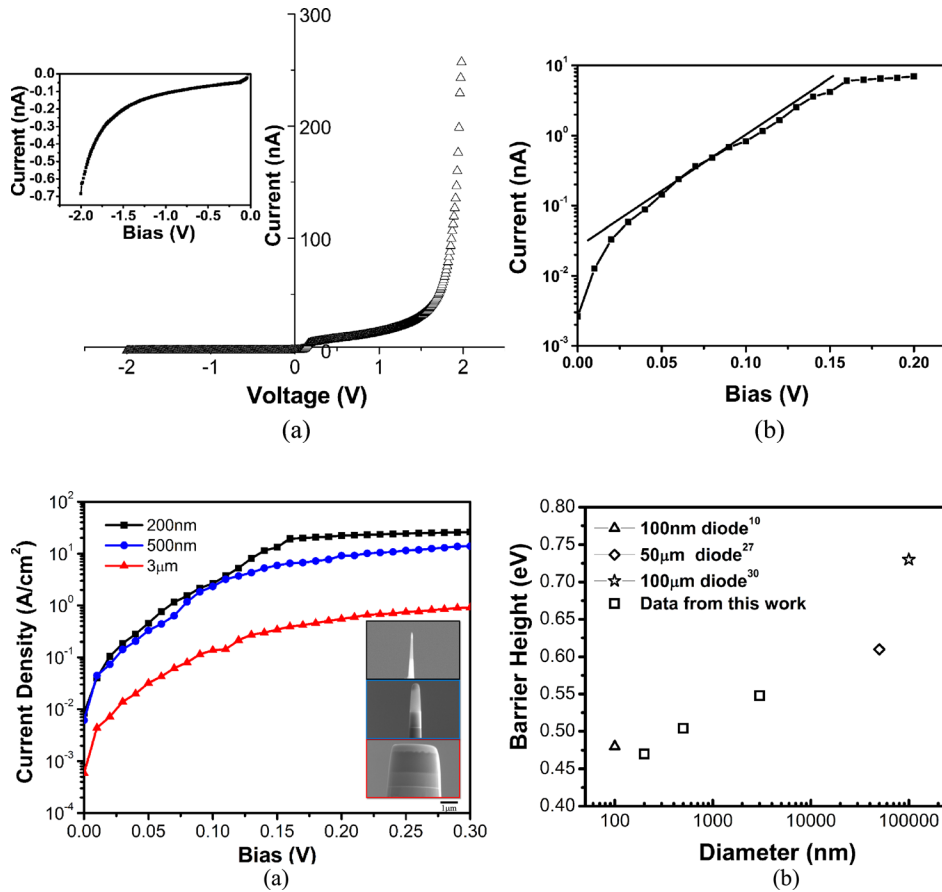


FIG. 3. (a) I-V characteristics of Pt/ZnO nanoneedle Schottky diode with a diameter of 200 nm. Inset shows the reverse current in detail; and (b) I-V curve of Pt/ZnO Schottky diode under forward bias condition and the fitting plot in thermionic-field emission regime.

to a higher barrier height for the larger diodes. The second explanation is that the variation in barrier height results from the joule heating effect. As the diameter of the diodes decreases, the degree of local heating increases, thereby decreasing the effective barrier height governed by thermoionic emission.^{31,32} Indeed, a lower barrier height was observed in smaller diameter nanowires.¹⁰ Liu³³ and Bui³⁴ performed 2-terminal thermal conductivity measurements using ZnO nanowires with diameter in the range of 70 to 200 nm. In the experiments, the thermal conductivity of nanowires was decreased by an order of magnitude in comparison with that of the bulk. This arises from a size dependent Joule heating effect that locally increases the temperature of nanoscale diodes. Other factors, including surface defects and leakage current through the edge of ZnO, are not considered as plausible explanations. In our experiments, the ideality factors were 1.11, 1.13, and 1.22 for 200 nm, 500 nm, and 3 μ m, respectively. The ideality factors of all diodes were close to 1, implying that a low concentration of defects or traps are present at the Pt/ZnO interface. The low ideality factors found in the nanoneedle Pt/ZnO diodes, therefore, suggest that the effect of surface defects is not significant. The edge leakage current is not a feasible origin of the effect, because a low conductivity depletion layer is formed near the surface of ZnO due to the adsorbed surface oxygen, which captures the free electrons in the ZnO.³⁵⁻³⁷

In conclusion, a test platform was fabricated that enables simple size-dependent electrical and structural characterization of nano-scale planar hetero-junction interfaces. The rectifying properties and low ideality factors measured from each sample indicate that the nanoneedle structure is an

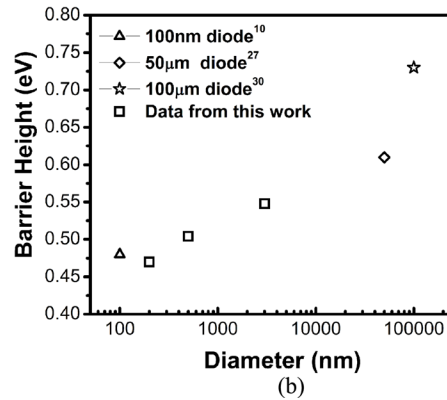


FIG. 4. (a) Plots of J vs V for different diameter Pt/ZnO nanoneedle Schottky diodes. Inset shows the SEM images of different size diodes; and (b) barrier heights as a function of size of diode (included with results from Heo,¹⁰ Ip,²⁷ and Oh³⁰ for comparison).

attractive candidate to probe nano-scale heterojunction interfaces. The diameter dependent barrier height was rationalized based on Joule heating effects resulting from size dependent thermal conductivity in ZnO and barrier height inhomogeneity over the Pt/ZnO contact area. The nanoneedle structure allows for exploration of various phenomena associated with charge transfer at hetero-junction interfaces, making it an attractive geometry to study size-dependent properties in optical and electronic devices.

We gratefully acknowledge financial support from the following: S.M. was supported by US DOE-BES Grant No. DEFG02-05ER46217 and D.A. was supported by the US NSF Grant No. 1254406. The research was carried out in part in the Frederick Seitz Materials Research Laboratory Central Facilities, University of Illinois.

¹D. C. Look, *Mater. Sci. Eng. B* **80**, 383 (2001).

²Y. I. Alivov, E. V. Kalinina, A. E. Cherenkov, D. C. Look, B. M. Ataev, and A. K. Omaev, *Appl. Phys. Lett.* **83**, 4719 (2003).

³A. Tsukazaki, A. Ohtomo, T. Onuma, M. Ohtani, T. Makino, M. Sumiya, K. Ohtani, S. F. Chichibu, S. Fukai, Y. Segawa, H. Ohno, H. Koinuma, and M. Kawasaki, *Nature Mater.* **4**, 42 (2005).

⁴D. C. Look, J. W. Hemsky, and J. R. Sizelove, *Phys. Rev. Lett.* **82**, 2552 (1999).

⁵Q. Wan, Q. H. Li, Y. J. Chen, T. H. Wang, X. L. He, J. P. Li, and C. L. Lin, *Appl. Phys. Lett.* **84**(18), 3654 (2004).

⁶X. D. Wang, C. J. Summers, and Z. L. Wang, *Nano Lett.* **4**(3), 423 (2004).

⁷K. B. Sundaram and A. Khan, *Thin Solid Films* **295**(1-2), 87 (1997).

⁸N. W. Emanetoglu, J. Zhu, Y. Chen, J. Zhong, Y. M. Chen, and Y. C. Lu, *Appl. Phys. Lett.* **85**(17), 3702 (2004).

⁹K. Nomura, H. Ohta, K. Ueda, T. Kamiya, M. Hirano, and H. Hosono, *Science* **300**(5623), 1269 (2003).

¹⁰Y. W. Heo, L. C. Tien, D. P. Norton, S. J. Pearton, B. S. Kang, F. Ren, and J. R. LaRoche, *Appl. Phys. Lett.* **85**(15), 3107 (2004).

¹¹S. N. Das, J. H. Choi, J. P. Kar, K. J. Moon, T. I. Lee, and J. M. Myoung, *Appl. Phys. Lett.* **96**, 092111 (2010).

¹²E. Koren, N. Berkovitch, O. Azriel, A. Boag, Y. Rosenwaks, and E. R. Hemesath, *Appl. Phys. Lett.* **99**, 223511 (2011).

¹³M. Law, L. E. Greene, J. C. Johnson, R. Saykally, and P. D. Yang, *Nature Mater.* **4**(6), 455 (2005).

¹⁴K. S. Leschkies, R. Divakar, J. Basu, E. Enache-Pommer, J. E. Boercker, C. B. Carter, U. R. Kortshagen, D. J. Norris, and E. S. Aydil, *Nano Lett.* **7**(6), 1793 (2007).

¹⁵L. E. Greene, M. Law, D. H. Tan, M. Montano, J. Goldberger, G. Somorjai, and P. D. Yang, *Nano Lett.* **5**(7), 1231 (2005).

¹⁶T. J. Hsueh, C. L. Hsu, S. J. Chang, and I. C. Chen, *Sens. Actuators, B* **126**(2), 473 (2007).

¹⁷Y. S. Zhang, K. Yu, D. S. Jiang, Z. Q. Zhu, H. R. Geng, and L. Q. Luo, *Appl. Surf. Sci.* **242**(1–2), 212 (2005).

¹⁸X. M. Zhang, M. Y. Lu, Y. Zhang, L. J. Chen, and Z. L. Wang, *Adv. Mater.* **21**(27), 2767 (2009).

¹⁹J. M. Luther, J. Gao, M. T. Lloyd, O. E. Semonin, M. C. Beard, and A. J. Nozik, *Adv. Mater.* **22**(33), 3704 (2010).

²⁰R. Ghosh and D. Basak, *Appl. Phys. Lett.* **90**(24), 243106 (2007).

²¹W. Lu and C. M. Lieber, *Nature Mater.* **6**(11), 841 (2007).

²²J. B. K. Law and J. T. L. Thong, *Appl. Phys. Lett.* **88**, 133114 (2006).

²³B. J. Jin, S. Im, and S. Y. Lee, *Thin Solid Films* **366**, 107 (2000).

²⁴K. Ip, G. T. Thaler, H. Yang, S. Y. Han, Y. J. Li, D. P. Norton, S. J. Pearton, S. Jang, and F. Ren, *J. Cryst. Growth* **287**, 149 (2006).

²⁵L. J. Brillson and Y. C. Lu, *J. Appl. Phys.* **109**, 121301 (2011).

²⁶F. Claeysens, A. Cheesman, S. J. Henley, and M. N. R. Ashfold, *J. Appl. Phys.* **92**(11), 6886 (2002).

²⁷K. Ip, Y. W. Heo, K. H. Baik, D. P. Norton, S. J. Pearton, S. Kim, J. R. LaRoche, and F. Ren, *Appl. Phys. Lett.* **84**, 2835 (2004).

²⁸S. K. Cheung and N. W. Cheung, *Appl. Phys. Lett.* **49**, 85 (1986).

²⁹S. M. Sze and K. K. Ng, *Physics of Semiconductor Devices*, 3rd ed. (John Wiley & Sons, Inc, Hoboken, New Jersey, 2007).

³⁰M. S. Oh, D. K. Hwang, J. H. Lim, Y. S. Choi, and S. J. Park, *Appl. Phys. Lett.* **91**, 042109 (2007).

³¹M. W. Allen, X. J. Weng, J. M. Redwing, K. Sarpatwari, S. E. Mohney, H. Von Wenckstern, M. Grundmann, and S. M. Durbin, *IEEE Trans. Electron Devices* **56**(9), 2160 (2009).

³²E. Gur, S. Tuzemen, B. Kilic, and C. Coskun, *J. Phys: Condens. Matter* **19**, 196206 (2007).

³³Y. Liu, Z. Y. Zhang, X. L. Wei, Q. Li, and L. M. Peng, *Adv. Funct. Mater.* **21**(20), 3900 (2011).

³⁴C. T. Bui, R. G. Xie, M. R. Zheng, Q. X. Zhang, C. H. Sow, B. W. Li, and J. T. L. Thong, *Small* **8**(5), 738 (2012).

³⁵C. Soci, A. Zhang, B. Xiang, S. A. Dayeh, D. P. R. Aplin, J. Park, X. Y. Bao, Y. H. Lo, and D. Wang, *Nano Lett.* **7**(4), 1003 (2007).

³⁶Q. H. Li, T. Gao, Y. G. Wang, and T. H. Wang, *Appl. Phys. Lett.* **86**, 123117 (2005).

³⁷J. D. Prades, R. J. Diaz, F. H. Ramirez, L. F. Romero, T. Andreu, A. Cirera, A. R. Rodriguez, A. Cornet, J. R. Morante, S. Barth, and S. Mathur, *J. Phys. Chem. C* **112**, 14639 (2008).